

A Novel Concept for Transformer Volt Second Balancing of a VIENNA Rectifier III Based on Direct Magnetizing Current Measurement

Franz Stögerer Johann W. Kolar Uwe Drofenik

Technical University Vienna
Dept. of Electrical Drives and Machines
Power Electronics Group
Gusshausstrasse 27/372
A-1040 Vienna, AUSTRIA / Europe
Tel. +43-1-58801-37225
Fax, +43-1-58801-37299
E-mail: fstoegerer@icam.tuwien.ac.at

ABSTRACT

For a VIENNA Rectifier III different turn-on and turn-off delay times of the power transistors and different on-state voltages of the valves would cause an unbalance of the positive and negative volt seconds applied to the high frequency transformer within a pulse period and/or result in transformer saturation without additional measures.

This paper proposes a novel concept for actively ensuring a symmetric magnetization with switching frequency of the transformer magnetic core of a VIENNA Rectifier III based on direct measurement of the magnetizing current. The magnetizing current is determined by subtraction of the transformer primary and the secondary currents being weighted according to the transformer turns ratio. The subtraction is realized by magnetic compensation employing a through-hole DC current transducer. A deviation from a symmetric magnetization within a pulse period is detected and used by a controller for closed-loop balancing of the volt seconds applied to the transformer primary in order to eliminate an existing asymmetry. The controller is designed based on sampled data system theory. The theoretical considerations and the controller dimensioning are verified by experimental results gained from a 8.5kW prototype of the VIENNA Rectifier III.

Keywords: VIENNA Rectifier, Transformer Volt Second Balancing, Transformer Magnetizing Current.

1 Introduction

In [1] a novel single-stage three-phase PWM rectifier system with sinusoidal input currents and high-frequency isolated and controlled output voltage has been introduced (cf. Fig.1(a)). As shown in Fig.1(b) segments of the AC-side line-to-line voltage are applied to the transformer primary winding. The secondary side voltage is rectified and filtered by a low-pass filter L_O, C_O . For suppressing switching frequency harmonics of the rectifier input current $i_{U,i}$ which is formed by pulse-width modulated segments of the transformed output current an input filter has to be employed. This results in a sinusoidal time-behavior of the current drawn from mains. The magnetization of the transformer ideally is symmetric and with pulse frequency, i.e. no low-frequency components are present under the assumption of ideal components.

However, in practice the power semiconductor on-state voltages, ohmic losses, finite transistor turn-off times, delay-times of the transistor gate drive circuits and the ripple of the

input filter capacitor voltage cause a deviation of the actual voltage applied to the transformer primary side from the ideal voltage shape which is assumed for the calculation of the relative on-times of the power transistors in order to guarantee a transformer volt seconds balance. A consideration of the parasitic effects in the course of the calculation of the transistor on times is not possible due to the dependence of the components on the system load state, junction temperature etc. Therefore, the transformer primary voltage contains besides pulse-frequency components also low-frequency harmonics that may cause saturation of the transformer magnetic core.

A symmetrization of the magnetization by passive means, i.e., by the insertion of ohmic resistors and/or by an artificial increase of parasitic resistances of the wiring is not possible and/or sufficient for high power and highly efficient systems [2].

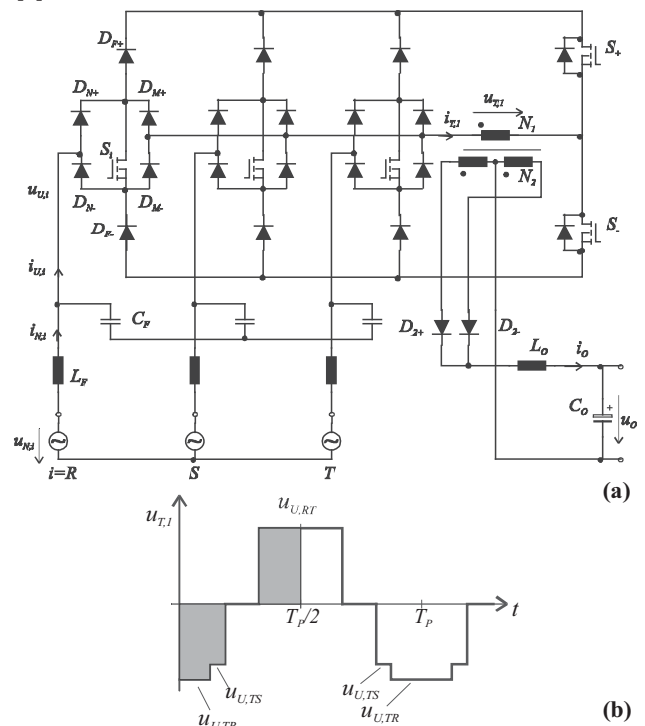


Fig.1: (a) Power circuit of the VIENNA Rectifier III and (b) local time-behavior of the transformer primary voltage $u_{T,1}$ (T_P denotes a pulse period), the balance of the positive and negative volt seconds applied to the transformer primary within a pulse half period is pointed out by dotted areas.

Inserting an air-gap in the transformer core would result in an increase of the maximum tolerable magnetizing current [3], which would reduce the resistance values required for a passive symmetrization. However, a magnetizing current being too high in magnitude results in a significant low-frequency harmonic distortion of the mains current and in an increase of the conduction losses of the power semiconductors.

Alternatively, as proposed in [3] (cf. pp. 320-322), [4] a blocking capacitor could be connected in series with the transformer primary for blocking any low-frequency components of the transformer primary voltage. The voltage which then actually is applied to the transformer primary winding does only contain components with switching frequency. However, as has become clear by a closer experimental analysis of this concept, a resonance between the main inductance of the transformer and the blocking capacitor might occur.

As described in [4], [5] also hall-sensors or small inductors could be employed for a direct measurement of the transformer magnetic flux. However, aiming for low manufacturing effort in the case at hand the application of such concepts is not feasible.

In this paper a novel concept for guaranteeing a symmetric magnetization of the high-frequency transformer of the VIENNA Rectifier III is presented [6]. There, the magnetizing current is determined by subtracting the transformer secondary current and the transformer primary current being weighted according to the transformer turns ratio. The subtraction which is performed by mutual magnetic compensation, i.e. by a DC current transducer, results in a signal which is used as input of a closed loop magnetizing current control which guarantees a symmetric transformer magnetization by properly changing the local average value of the transformer primary voltage.

2 Direct Measurement of the Transformer Magnetizing Current

As described above the magnetizing current is measured by subtraction of the weighted transformer primary and secondary currents. The subtraction is performed directly by using a through-hole DC current transducer. There, the turns ratio has to be chosen according to the transformer turns-ratio (in the case at hand 6:1). For high-power systems the increase of the total component costs due to the sensing of the magnetizing current is marginal in comparison to the gained increase of system performance and reliability. The concept also allows to keep the safety margin considered in the transformer core dimensioning low and therefore helps to reduce the transformer realization effort.

In Fig.2 (a) the configuration for measuring of the magnetizing current using a through-hole DC current transformer is shown in connection with the transformer equivalent circuit. Figure 2(b) depicts the time-behavior of transformer primary current, the transformer secondary current and the resulting magnetizing current.

Remark: In case of a non-integer turns transformer ratio N_1/N_2 the primary current can be measured by an AC-current sensor with a turns ratio $i_1/i_2=N_1/N_2$. The output current of the AC-current sensor and the secondary current $i_{T,2}$ are then compensated by $n_1=n_2=1$ for the magnetizing current sensor.

The following discussion is based on the magnetizing current $i_m = i_m'' \cdot N_2/N_1$ referred to the primary side.

3 Control of the Magnetizing Current

Before analyzing the structure of the magnetizing current controller in detail a short description of the control of the VIENNA Rectifier III is given.

Because of the complexity of the system and/or the high computational effort for calculating the switching times of the power transistors the control of the system is performed by a digital signal processor (ADSP 21061). During each pulse half period ($1/2T_p = 16\mu s$) the DSP takes samples of the input voltages and the output voltage of the converter and computes the turn-on times of the power transistors S_i ($i=1,2,3,+,-$) under consideration of a pulse-frequency symmetric magnetization of the transformer and a sinusoidal guidance of the rectifier input currents. Since the measurement of the input values and the computation of the turn-on times takes about $10\mu s$ the calculated switching times are available at the end of the actual pulse half period and, therefore, are applied within the next pulse half period. The calculated duration of the on-times of the switches are transformed into gate-signals of the power transistors [1] by three PWM output stages (implemented by a PLD, ALTERA EPM 7128) and a logic circuit (realized by an EPROM).

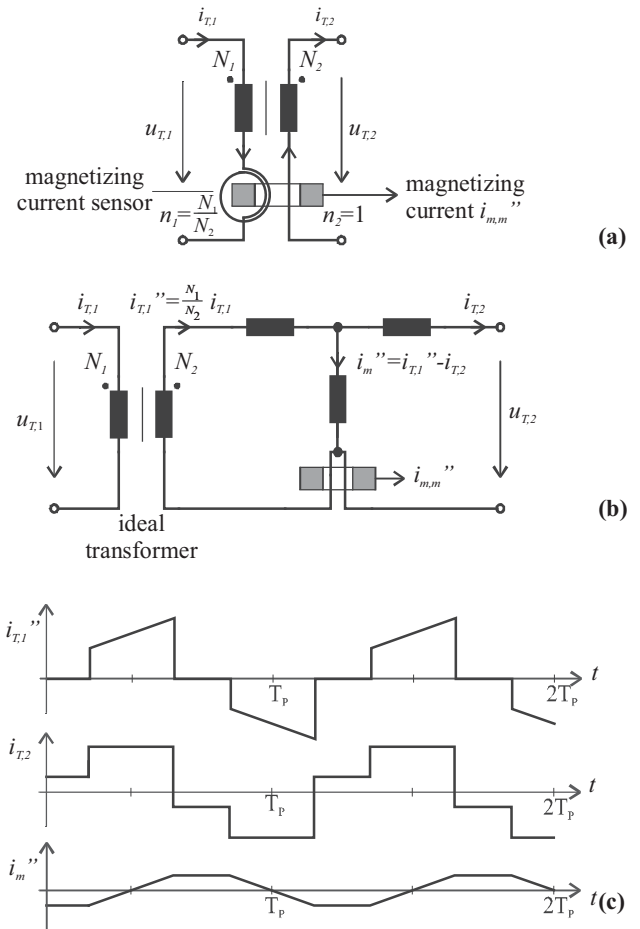


Fig.2: Direct measurement of the magnetizing current of a transformer by using a DC current transducer, $n_1=N_1/N_2$, $n_2=1$ (shown for $n_1=2$, $n_2=1$) (a), equivalent circuit and magnetizing current sensor (b), time behavior of primary current, secondary current and (c). magnetizing current i_m'' (referred to the secondary side).

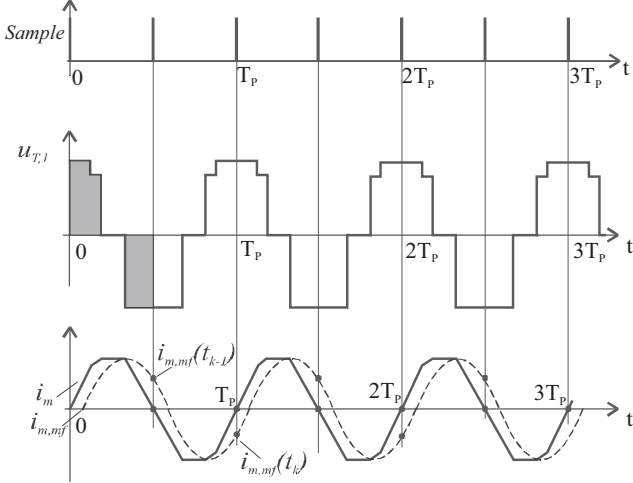


Fig. 3: Sampling time instants, transformer primary voltage $u_{T,1}$, resulting magnetizing current i_m and time behavior of the filtered magnetizing current $i_{m,mf}$.

3.1 Control Structure

For the control of the magnetization of the transformer the value of the magnetizing current at the end of each pulse half period $i_m(t_k)$ ($t_k = k \cdot 1/2 T_p$, $k=1,2,3..$) is needed because in case of symmetric magnetization of the transformer the magnetizing current equals zero at these time instants independent of the degree of modulation or dynamic changes (see Fig. 3). In case of asymmetric magnetization of the transformer the values of $i_m(t_k)$ are not equal to zero and follow the integrated DC component of the applied transformer voltage. (Theoretically, the sampling of the magnetizing current at different time instants is possible too, although the actual degree of modulation has to be considered in that case.) The sampling of the magnetizing current at the end of each pulse half period shows the advantage of no switching actions occurring at these times. This significantly reduces the influence of disturbances on the measured values of the magnetizing current.

The value of the magnetizing current at the end of each pulse half period is sampled and used for calculating the switching pattern of the next pulse half period. The input current shape of the VIENNA Rectifier III is not influenced by this scheme because of the existence of two redundant rectifier input current space vectors with opposite magnetization effect on the

transformer. According to the measured magnetization of the transformer the distribution of the on-times of these two redundant input current space vectors is defined.

The value of the magnetizing current at the end of a pulse half period can be derived by two methods which are introduced in the following.

3.1.1 Sampling of the Magnetizing Current (Method 1)

The simplest way for measuring the magnetization of the transformer is sampling of the output signal of the magnetizing current sensor $i_{m,m}$ at each pulse half period ($t_k = k \cdot 1/2 T_p$, $k=1,2,3..$). The cut-off frequency of the magnetizing current sensor causes a delay of the measured signal compared to the actual magnetizing current resulting in an error of the sampling value. For $i_m(t_k) = 0$ a sampling value $i_{m,m}(t_k) \neq 0$ occurs (Fig. 3).

Furthermore, the fast change of the potential of the primary and secondary transformer windings and the capacitive coupling and/or the high frequency behavior of the magnetizing current sensor [7] result in spurious signals distorting the measured value $i_{m,m}$. Therefore, sampling of the signal could be falsified. To reduce the spurious signals the output signal of the magnetizing current sensor has to be filtered by a low-pass filter giving the signal $i_{m,mf}$. This low-pass filter causes a further delay of the measured signal and, therefore, an increased error of the sampling scheme.

The time-behavior of the magnetizing current shows opposite slope for two subsequent sampling time instants. Therefore, the average value of two subsequent samples ($i_{m,mf}(t_{k-1}) + i_{m,mf}(t_k)$) is zero. The DSP therefore uses the average value of the last two samples ($i_{m,mf}(t_{k-1})$, $i_{m,mf}(t_k)$) for correction of the low-frequency component of the transformer primary voltage. If no averaging of the sample values is performed a variation of the controller output signal occurs for subsequent pulse half periods.

Fig. 4 shows the block diagram of the magnetizing current control. For the sake of simplicity the leakage inductance of the transformer and the ohmic resistances are neglected. The transformer is defined by its main inductance L_H . Here, the symbol \bar{x} means the local averaging of the value x during one sampling period $T = T_p/2$.

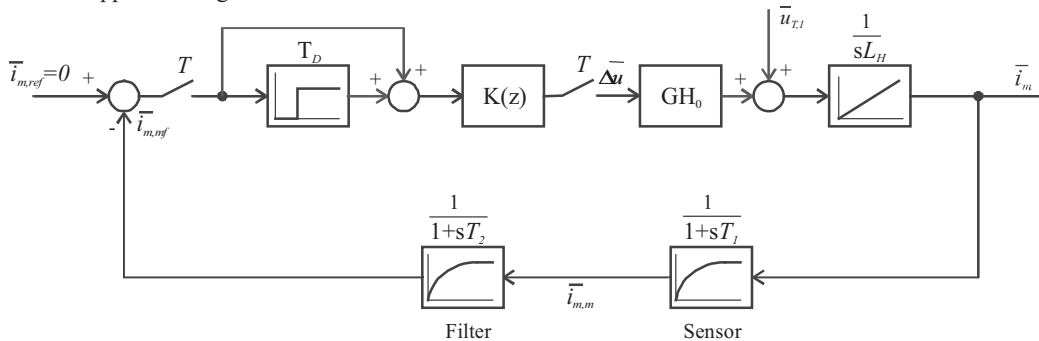


Fig. 4: Block diagram of the control of the transformer magnetizing current based on the sampling of the magnetizing current (method 1). The averaging of the last two sample values is performed by a dead time $T_D = T = T_p/2$ and addition with the non-delayed value. The transfer function $K(z) = 1/2 K 1/z$ considers the factor $1/2$ for averaging of the last two sample values, the proportional gain constant K of the magnetizing current controller, and the dead time T defined by the signal processing time of the DSP. The controlled system consists of only the transformer main inductance L_H (integrator $1/sL_H$) neglecting the leakage inductance of the transformer and the ohmic resistances for the sake of simplicity. Furthermore, a PT1-element representing the transfer function of the magnetizing current sensor and a PT1-element representing the filtering of the sensor signal are considered.

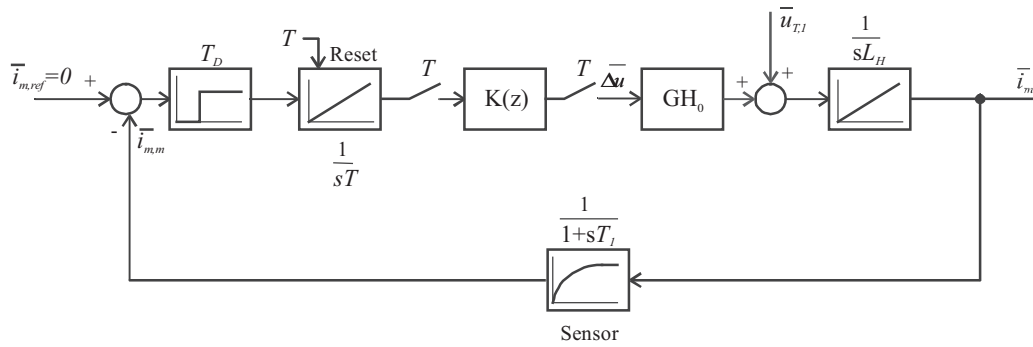


Fig. 5: Block diagram of the transformer magnetizing current controller for integration of the magnetizing current in sections (method 2). The averaging is performed via a resettable integrator. Because the integration has to be performed symmetrically around the time instants $t_k = k \cdot 1/2 T_p$, $k=1,2,3\dots$ a delay of $T_D = 1/2 T = 1/4 T_p$ of the measured magnetizing current is necessary. The controller $K(z) = K/z$ comprises the proportional gain constant K of the controller and the dead time T according to the signal processing time of the DSP.

3.1.2 Integration of the Magnetizing Current in Sections (Method 2)

For improved interference suppression concerning the magnetizing current at the sampling time instants averaging by integration in sections [8] can be applied. As shown in Fig. 6, two resettable integrators (A, B) with according sample-and-hold elements (C, D) are used. The two integrators are controlled in a way that always one integrator integrates the measured magnetizing current symmetrically around the zero line (forming the average value during that time period, therefore), while the output value of the other integrator is stored in the sample-and-hold element, to be activated afterwards.

The two integrators act alternately so that the output value of one integrator is always stored and available for further calculations while the other integrator forms the average value.

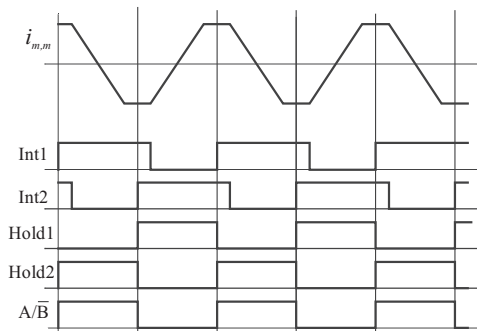
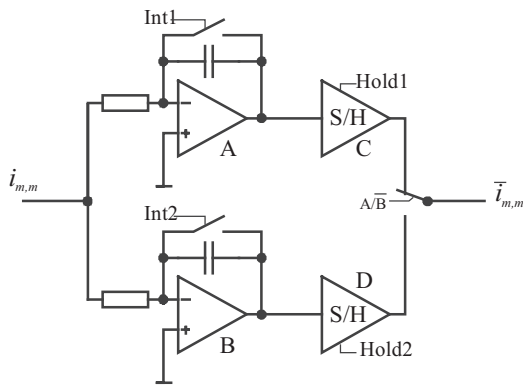


Fig. 6: Circuit for integration of the magnetizing current in sections (a) and control signals (b)

A delay of the measured signal according to the time constant of the measurement $1/2 T = 1/4 T_p$ is necessary because the integration of the measured magnetizing current has to be done symmetrically to the sampling time instants.

As shown in Fig. 7 the integration of the measured magnetizing current covers two calculation time intervals of the DSP. In case of load variations and/or changes of the degree of modulation this can result in a local error of the calculated magnetization of the transformer. This is a basic drawback of method 2.

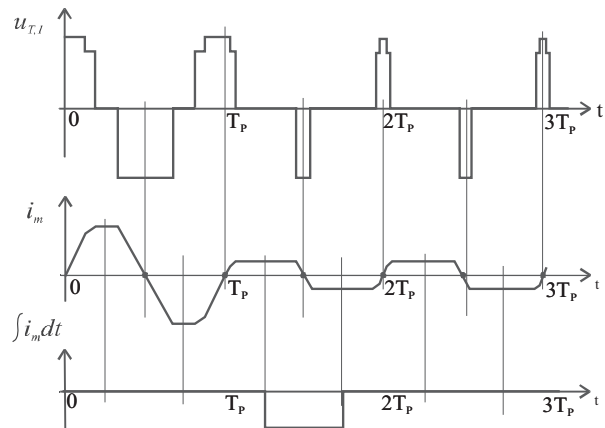


Fig. 7: Time behavior of the integration of the magnetizing current in sections (method 2) for a step change of the degree of modulation.

(a)

3.2 Controller design

3.2.1 Sampling of the Magnetizing Current (Method 1)

The z-transformation of the control circuit shown in Fig. 4 gives the following transfer function of the open loop:

$$F_O(z) = \frac{K}{2} \cdot \frac{z+1}{z^2} \cdot \frac{1}{L_H} \cdot \left(A + \frac{B \cdot T}{z-1} + C \cdot \frac{z-1}{z - e^{-T/T_1}} + D \cdot \frac{z-1}{z - e^{-T/T_2}} \right) \quad (1)$$

$$\text{with } A = -(T_1 + T_2), \quad B = 1, \quad C = \frac{T_1^2}{T_1 - T_2}, \quad D = \frac{-T_2^2}{T_1 - T_2} \quad (2)$$

Figure 8 shows the root-locus diagram (for $L_H=3mH$, $T_I=1\mu s$ and $T_2=3\mu s$) in the z-plane and the root-locus diagram transformed back into the w-plane employing the Tustin-approximation [9], [10] showing curves of constant damping. The limit of stability is reached for a proportional gain constant of $K=143$ V/A.

As shown in Fig. 8 (b) the controller design can be based on a dominant pole pair. To achieve a minimum control error the amplification of the controller should be as high as possible. With increasing amplification however also settling time and overshoot will increase. As a compromise the damping of the dominant substitute-PT2-element is chosen with $D=0.5$ which results (according to Fig. 8(b)) in a proportional gain constant of $K=56$ V/A.

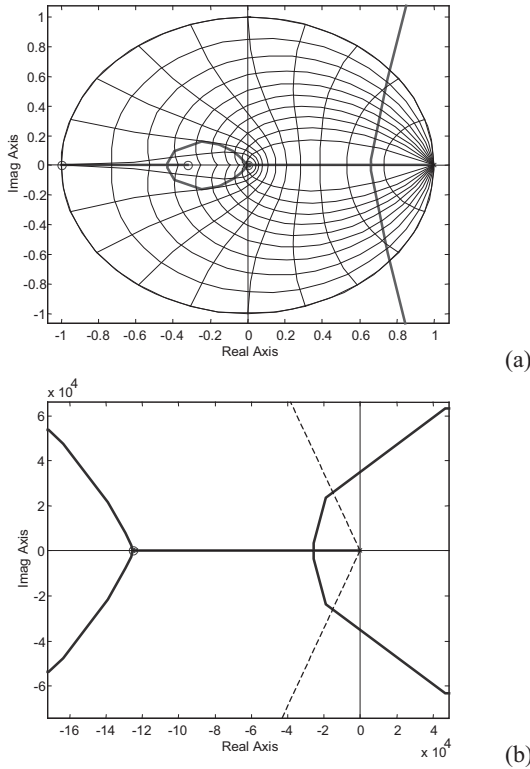


Fig.8: Root-locus diagram of the z-transformation (a) and root-locus diagram transformed back into the w-plane employing the Tustin-approximation (b) of the magnetizing current controller for sampling of the magnetizing current (method 1). The dashed line in (b) indicates constant damping $D=0.5$.

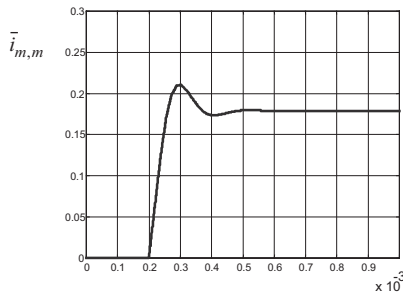


Fig.9: Disturbance transfer function of the magnetizing current controller for sampling of the magnetizing current (method 1) with a controller gain of $K=56$ V/A for a disturbing step function of $\bar{u}_{T,1} = 10V$.

According to practical investigations within one pulse period a maximum DC component of the transformer primary voltage of 10V can occur. **Figure 9** shows the disturbance transfer function for a disturbance step of $u_{T,1} = 10V$ and a controller gain of $K=56$ V/A. The use of a simple proportional controller results in a stationary control error of 0.18A. The settling time is 0.45ms and the maximum control error is 0.21A in this case. For a maximum value of the magnetizing current $\hat{i}_m = 1.66A$ this is a relative error of 12.6% and therefore acceptable.

3.2.2 Integration of the Magnetizing Current in Sections (Method 2)

Since the required dead time T_D is equal to the half sampling time T the dead time cannot be described as polynomial function of z . The dead time has to be implemented in form of a Padé-approximation ($T_2=T_D/2$). The z-transformation of the control circuit of Fig.5 gives the following transfer function of the open loop:

$$F_O(z) = K \cdot \frac{z-1}{z^2} \cdot \frac{1}{L_H \cdot T} \left(A + \frac{B \cdot T}{z-1} + C \cdot \frac{T^2}{(z-1)^2} + D \cdot \frac{z+1}{z-e^{-\frac{T}{T_1}}} + E \cdot \frac{z-1}{z-e^{-\frac{T}{T_2}}} \right) \quad (3)$$

$$\text{with } A = T_1^2 + 2T_1T_2 + 2T_2^2, B = -T_1 - 2T_2, C = 1, D = \frac{-2 \cdot T_1^3}{T_1 - T_2} + T_1^2, E = \frac{T_2^3}{T_1 - T_2} \quad (4)$$

Figure 11 shows the root-locus diagram (for $L_H=3mH$, $T_I=1\mu s$ and $T_2=T_D/2=4\mu s$) in the z-plane and the root-locus diagram transformed back into the w-plane employing the Tustin-approximation [9], [10] showing curves of constant damping. The limit of stability is reached for a proportional gain constant of $K=117$ V/A.

As in case of method 1 the controller design can be based on a dominant pole pair. As before, the damping is chosen with $D=0.5$ which results (according to Fig. 11(b)) in a proportional gain constant of $K=48$ V/A.

Figure 10 shows the disturbance transfer function for a disturbance step of $u_{T,1} = 10V$ and a controller gain of $K=48$ V/A. The use of a simple proportional controller results in a stationary control error of 0.21A. The settling time is 0.44ms and the maximum control error is 0.24A in this case. For a maximum value of the magnetizing current $\hat{i}_m = 1.66A$ this is an acceptable relative error of 14.5%.

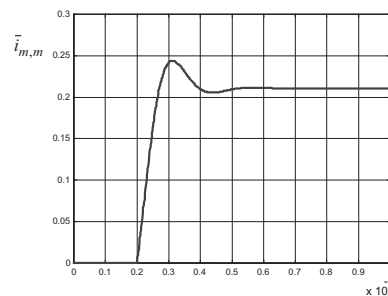


Fig.10: Disturbance transfer function of the magnetizing current controller for integration of the magnetizing current in sections(method 2) with a controller gain of $K=48$ V/A for a disturbing step function of $\bar{u}_{T,1} = 10V$.

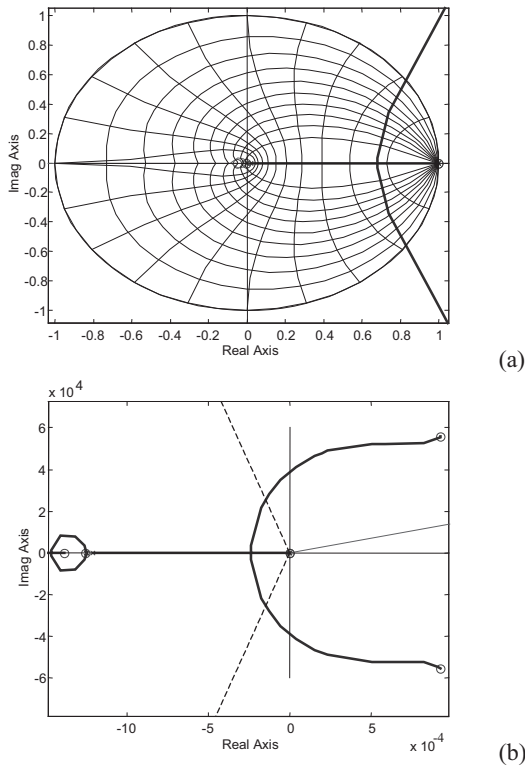


Fig.11: Root-locus diagram of the z-transformation (a) and root-locus diagram transformed back into the w-plane employing the Tustin-approximation (b) of the magnetizing current controller for integration of the magnetizing current in sections (method 2). The dashed line in (b) describes constant damping $D=0.5$.

4 Experimental Results

The experimental results are based on a laboratory prototype with the following parameters:

Input voltage:	$U_N = 400$ V(line-to-line)
Output voltage:	$U_O = 48$ V
Output power:	$P_O = 8.5$ kW
Switching frequency:	$f_P = 31.25$ kHz
Transformer main inductance:	$L_H = 3$ mH.

The behavior of the system with and without i_m – controller is investigated and compared. Therefore, the experiments are performed under reduced input voltage $U_N=280$ V and reduced output power $P_O=1$ kW.

To measure the magnetizing current a through-hole DC current transformer CSNP661 from Honeywell has been used. **Figure 12** shows the magnetizing current measured by this current transformer and further current signals derived by low-pass filtering and/or averaging. The phase shift caused by low-pass filtering of the measured signal is obvious. This phase shift is compensated by averaging done by the DSP (see Fig. 3).

The system behavior for a step change of the local average value of the transformer primary voltage of 10V is shown in **Fig. 13**. The average value of the magnetizing current is measured by integration in sections (as described in section 3.1.2).

The experimental results are in good agreement with the simulated step responses shown in Fig. 9 and Fig. 10.

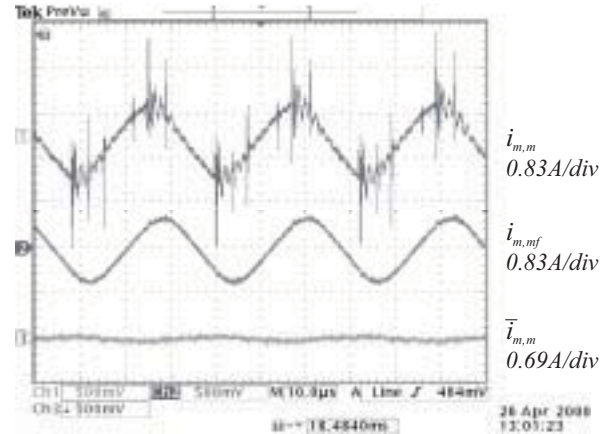


Fig.12: Output signal of the magnetizing current transducer $i_{m,m}$, the low-pass-filtered signal $i_{m,mf}$ and the locally averaged signal $\bar{i}_{m,m}$.

In **Fig. 14** the effect of the magnetizing current controller is demonstrated. Without active control the time behavior of the magnetizing current shows a low frequency component of high amplitude. Employing a magnetizing current controller the magnetizing current can be held close to zero line.

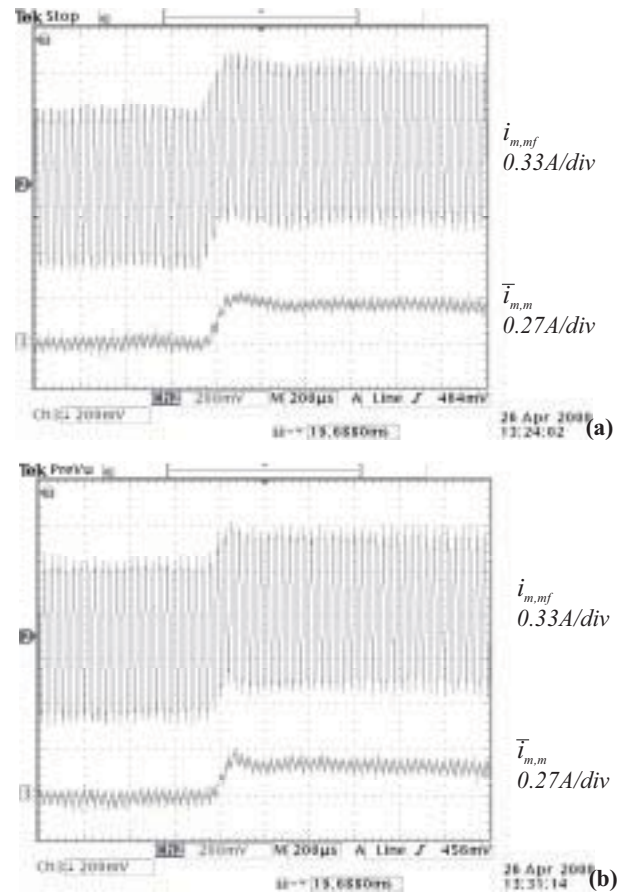


Fig.13: Step response of the magnetizing current for a step change of the disturbance voltage $u_{T,1}=10$ V and control of the magnetizing current with sampling of the magnetizing current (method 1) (a) and integration in sections (method 2) (b).

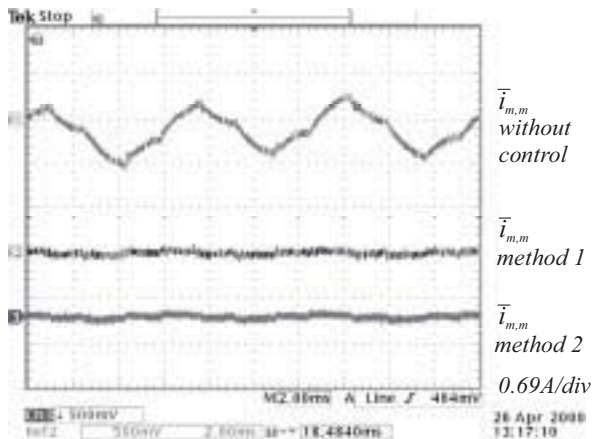


Fig.14: Time behavior of the magnetizing current without (top) and with (bottom) magnetizing current controller.

5 Conclusions

Without active control of the magnetizing current there is the possibility of an unreliaibly high magnetizing current possibly resulting in a saturation of the transformer of the VIENNA Rectifier III. If methods are employed which allow higher magnetizing current and passive symmetrization, the increased magnetizing current distorts the ideal sinusoidal input current shape.

Measuring the magnetizing current employing a through-hole DC current transdfomer results in a signal $i_{m,m}$ sufficient for active symmetrization of the magnetization of the transformer although the measurement shows a relatively high noise level.

It was shown that a integrating measurement of the magnetizing current is not necessary and a simple sampling of the measured signal $i_{m,mf}$ is sufficient. Besides higher realization effort the integrating measurement of the magnetizing current information has the disadvantage of a temporary measurement error in case of changes of the degree of modulation.

For sampling of the magnetizing current it has to be considered that the sampling has to be performed within each pulse half period so that the delay time (resulting from the bandwidth limitation of the magnetizing current sensor and the filtering of the measured signal) of $i_{m,mf}$ compared to i_m does not result in an error when averaging the sampled signal values.

The described method can also be employed with DC-DC converter systems. In this case a series capacitor (generally restricting the dynamic behavior of the system) on the transformer primary side can be omitted and/or the magnetizing current can be kept low. The switching losses are reduced and/or the efficiency improved.

The higher costs of the magnetizing current transdfomer are neglectable for systems of higher power.

For employing the described method of magnetizing current control for a broader field of applications through-hole DC current transdfomers with large holes and relatively small instrument range would be advantageous.

Acknowledgment

The authors are very much indebted to the *Hochschuljubiläumsstiftung der Stadt Wien* for the generous support of the research of the Power Electronics Group of the Dept. of El. Drives and Machines at the Technical University of Vienna.

REFERENCES

- [1] **Kolar, J.W., Drofenik, U., Ertl, H., and Zach, F.C.:** *VIENNA Rectifier III – A Novel Three-Phase Single-Stage Buck-Derived Unity Power Factor AC-to-DC Converter System*. Proceedings of the Nordic Workshop on Power and Industrial Electronics, Espoo, Finland, Aug. 26-27, pp. 9-18 (1998).
- [2] **Wilson, D.:** *A New Pulsewidth Modulation Method Inherently Maintains Output Transformer Flux Balance*. Proceedings of the 8th International Solid-State Power Electronics Conference, Dallas (TX), April 27-30, pp. D-1/1 – D-1/15 (1981).
- [3] **Mohan, N., Undeland, T.M., and Robbins, W.P.:** *Power Electronics – Converters, Applications, and Design*. 2nd Edition, John Wiley & Sons, Inc. (1995).
- [4] **Klopper, S., and Ferreira, J.A.:** *A Sensor for Balancing Flux in Converters with a High Frequency Transformer Link*. Record of the 28th IEEE Industry Applications Society Annual Meeting, Toronto, Canada, Oct. 2-8, Pt. II, pp. 1315-1320 (1993).
- [5] **Patel, R.:** *Detecting Impending Core Saturation in Switched-Mode Power Converters*. Proceedings of the 7th National Solid-State Power Conversion Conference, pp. B-3/1 – B-3/11 (1980).
- [6] **Kolar, J.W.:** *Verfahren und Vorrichtungen zur Erfassung und Ausregelung eines Gleichanteiles des Magnetisierungsstromes von Hochfrequenz-Leistungstransformatoren in Stromrichterschaltungen*. Austrian Patent Application A1821/98, filed: Oct. 14, 1998.
- [7] **Pankau, J., Leggate, D., Schlegel, D., Kerkman, R., and Skibinski, G.:** *High Frequency Modelling of Current Sensors*. Proceedings of the 14th IEEE Applied Power Electronics Conference, Dallas, Vol. 2, March 14-18, pp. 788-794 (1999).
- [8] **Chin, T.H., Nakano, M., and Hirayama, T.:** *Accurate Measurement of Instantaneous Values of Voltage, Current and Power for Power Electronics Circuits*. Proceedings of the 29th IEEE Power Electroncis Specialists Conference, Fukuoka, Japan, May 17-22, Vol. 1, pp. 302-307 (1998).
- [9] **Duan, Y., Jin, H.:** *Digital Controller Design for Switchmode Power Converters*. Proceedings of the 14th IEEE Applied Power Electronics Conference, Dallas, March 14-18, Vol. 2, pp. 967-973 (1999).
- [10] MATLAB, The Math Works, Inc.